ORGANIC LETTERS

2011
Vol. 13, No. 6
1290–1293

Visualization of Nitroxyl in Living Cells by a Chelated Copper(II) Coumarin Complex

Yi Zhou, Ke Liu, Ju-Ying Li, Yuan Fang, Tian-Chu Zhao, and Cheng Yao*

State Key Laboratory of Materials-Oriented Chemical Engineering and College of Science, Nanjing University of Technology, Nanjing 210009, People's Republic of China

yaochengnjut@126.com

Received December 20, 2010

ABSTRACT

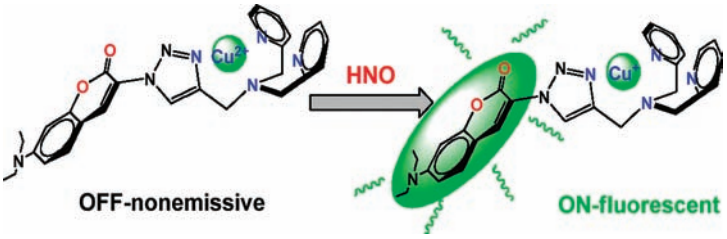

The coumarin-based probe Cu(II)-COT1 was successfully developed for the detection of HNO on the basis of the reduction reaction. In addition, highly selective "turn on" type fluorogenic behavior upon the addition of Angeli's salt ($Na_2N_2O_3$) was also applied to bioimaging in A375 cells.

Nitric oxide (NO) has received considerable attention due to its role as active signal-inducing messenger biomolecule in immune systems.[1] NO at a moderate concentration plays a critical role in physiological processes such as anticancer activity, vasodilation, synaptic activity, and neurotransmission.[2] Misregulation of NO production has been associated with pathological conditions such as cancer, ischemia, septic shock, inflammation, and neurodegeneration.[3] One of the nitrogen oxides relevant to biology is known as nitroxyl (HNO), which is the reduced/protonated form of the signaling agent nitric oxide (NO). HNO can be formed directly from nitric oxide synthase under the appropriate conditions.[4] Biologically, HNO also increases cardiac contractility in both normal and failing canine hearts through mechanisms that include increased sarcoplasmic reticulum calcium release and uptake and increased calcium dependent force development in cardiac tissue.[5] Thus, development of sensitive and selective methods for the detection of biological NO and HNO is of importance.

There are many techniques available for detecting NO and HNO, such as electrochemistry, colorimetry, electron paramagnetic resonance (EPR), and chemiluminescence.[6] However, these methods cannot be used to visualize NO and HNO in vitro and in vivo. Fluorescence analysis has high sensitivity and selectivity, and if it were to be

(1) (a) Palmer, R. M. J.; Ferrige, A. G.; Moncada, S. *Nature* **1987**, *327*, 524–526. (b) Butler, A. R.; Williams, D. L. H. *Chem. Soc. Rev.* **1993**, *22*, 233–241. (c) Murad, F. *Angew. Chem., Int. Ed.* **1999**, *38*, 1856–1868. (d) Furchgott, R. F. *Angew. Chem., Int. Ed.* **1999**, *38*, 1870–1880. (e) Zimmet, J. M.; Hare., J. M. *Circulation* **2006**, *114*, 1531–1544.

(2) (a) Xu, W.; Liu, L. Z.; Loizidou, M.; Ahmed, M.; Charles, I. G. *Cell Res.* **2002**, *12*, 311–320. (b) Hou, Y.; Wang, J.; Andreana, P. R.; Cantauria, G.; Tarasia, S.; Sharp, L.; Braunschweiger, P. G.; Wang, P. G. *Bioorg. Med. Chem. Lett.* **1999**, *9*, 2255–2256.

(3) (a) Tfelt-Hansen, J.; Ferreira, A.; Yano, S.; Kanuparthi, D.; Romero, J. R.; Brown, E. M.; Chattopadhyay, N. *Am. J. Physiol.* **2005**, *288*, E1206–E1213. (b) Lala, P. K. *Cancer Metastasis Rev.* **1998**, *17*, 1–6. (c) Nelson, E. J.; Connolly, J.; McArthur, P. *Biol. Cell* **2003**, *95*, 3–8.

(4) (a) Fukuto, J. M.; Dutton, A. S.; Houk, K. N. *ChemBioChem* **2005**, *6*, 612–619. (b) Hobbs, A. J.; Fukuto, J. M.; Ignarro, L. J. *Proc. Natl. Acad. Sci. U.S.A.* **1994**, *91*, 10992–10996.

(5) (a) Paolocci, N.; Saavedra, W. F.; Miranda, K. M.; Martignani, C.; Isoda, T.; Hare, J. M.; Espey, M. G.; Fukuto, J. M.; Feelisch, M.; Wink, D. A.; Kass, D. A. *Proc. Natl. Acad. Sci. U.S.A.* **2001**, *98*, 10463–10468. (b) Paolocci, N.; Katori, T.; St. Champion, H. C.; John, M. E.; Miranda, K. M.; Fukuto, J. M.; Wink, D. A.; Kass, D. A. *Proc. Natl. Acad. Sci. U.S.A.* **2003**, *100*, 5537–5542. (c) Dai, T. Y.; Tian, Y.; Tocchetti, C. G.; Katori, T.; Murphy, A. M.; Kass, D. A.; Paolocci, N.; Gao, W. D. *J. Physiol.* **2007**, *580*, 951–960. (d) Reisz, J. A.; Klorig, E. B.; Wright, M. W.; King, S. B. *Org. Lett.* **2009**, *11*, 2719–2721.

(6) (a) Malinski, T.; Taha, Z. *Nature* **1992**, *358*, 676–678. (b) Ridnour, L. A.; Sim, J. E.; Hayward, M. A.; Wink, D. A.; Martin, S. M.; Buettner, G. R.; Spitz, D. R. *Anal. Biochem.* **2000**, *281*, 223–229. (c) Nagano, T.; Yoshimura, T. *Chem. Rev.* **2002**, *102*, 1235–1269. (d) Hetrick, E. M.; Schoenfisch, M. H. *Annu. Rev. Anal. Chem.* **2009**, *2*, 409–433.

(7) (a) Zheng, H.; Shang, G. Q.; Yang, S. Y.; Gao, X.; Xu, J. G. *Org. Lett.* **2008**, *10*, 2357–2360. (b) Kojima, H.; Nakatsubo, N.; Kikuchi, K.; Kawahara, S.; Kirino, Y.; Nagoshi, H.; Hirata, Y.; Nagano, T. *Anal. Chem.* **1998**, *70*, 2446–2453. (c) Sasaki, E.; Kojima, H.; Nishimatsu, H.; Urano, Y.; Kikuchi, K.; Hirata, Y.; Nagano, T. *J. Am. Chem. Soc.* **2005**, *127*, 3684–3685. (d) Gabe, Y.; Urano, Y.; Kikuchi, K.; Kojima, H.; Nagano, T. *J. Am. Chem. Soc.* **2004**, *126*, 3357–3367. (e) Zhang, R.; Ye, Z.; Wang, G.; Zhang, W.; Yuan, J. *Chem. Eur. J.* **2010**, *16*, 6884–6891.

10.1021/ol103077q
Published on Web 02/15/2011

incorporated into a membrane-permeable probe, it could be used to detect NO and HNO at the cellular level. A number of groups have developed a variety of fluorescent probes for NO and HNO, and these have been partially successful for fluorescent imaging agents in living cells.[7−9,12] However, these probes have some undesirable characteristics related to their compatibility with living cells, pH-dependent fluorescence, water solubility, and membrane permeability.[10,8b] Membrane permeability is the key feature for imaging experiments in intact cells for which continual permeation of intracellular with artificial physiological conditions is required.[11] Fluorescein[12] and boron−dipyrromethene (BODIPY)[9] dyes have been designed as fluorophore platforms for the construction of efficient membrane-permeable probes. Coumarin and its derivatives are used extensively as fluorescence labeling reagents for their excellent photophysical properties of high fluorescence quantum yield and efficient membrane permeability.[13] Therefore, we designed a probe for nitroxyl (HNO) including a coumarin chromophore and a tripodal dipicolylamine receptor, which was attached via a triazole bridge. The receptor provides a rigid Cu(II) binding site spacer between the coumarin fluorophore and chelating ligand. This type of probe was previously reported by Lippard's group, and the aim of this work was to produce a probe with an improved response compared to their BODIPY probe. With the aid of Lippard's design strategy,[9] the probe also provides N bridges to minimize the distance between the Cu^{2+} binding site and coumarin fluorophore, which will ensure strong fluorescence quenching in the off state of Cu(II) coumarin. Upon interaction with HNO, chelated Cu(II) coumarin is reduced and the Cu(I) coumarin complex forms, which induces an increase in the fluorescence intensity. Changes in [HNO] under physiological conditions will exhibit "turn-on" type fluorogenic behavior, which can be detected by measuring the ratio of green fluorescence intensity with good sensitivity and selectivity.

The synthesis of coumarin−trizole (**COT1**) and a proposed mechanism are shown in Scheme 1. Diazotization of

Scheme 1. Synthesis of Coumarin−Trizole (**COT1**) and Proposed Mechanism of Interaction with HNO To Generate Fluorescence

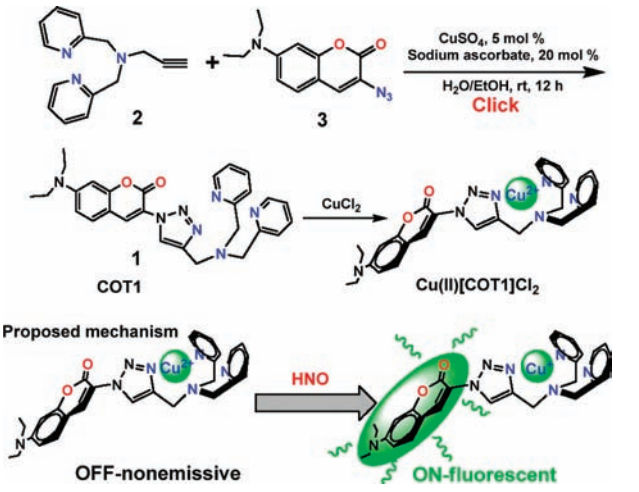

amino−coumarin with NaN_3 afforded azide−coumarin **3**, which was further installed by the copper(I)-mediated click cycloaddition[14] of alkyne **2** to give **COT1** in 63% yield. The chelated complex Cu^{II}[**COT1**]Cl_2 was easily prepared by addition of $CuCl_2$ to **COT1**. This complex was soluble and stable under physiological conditions in saline. **COT1** and Cu(I)-**COT1** are both green emission fluorophores, and they each displayed one absorption band in the visible region centered at 400 nm (**COT1**, 8.08×10^4 M^{-1} cm^{-1}) and 408 nm (Cu(I)-**COT1**, 8.15×10^4 M^{-1} cm^{-1}) (Figure S1, Supporting Information). Acid−base fluorescence titrations revealed that the fluorescence intensity of Cu(I)-**COT1**/Cu(II)-**COT1** was unaffected by pH values between 6.08 and 9.41 (excitation at 415 nm). This suggests that the probe would work well at physiological pH, although the fluorescence intensity of Cu(I)-**COT1** was quenched slightly at pH < 6.0 (Figures S2 and S3, Supporting Information).

The emission profile of **COT1** showed typical coumarin green fluorescence at 499 nm, with a high quantum yield ($\Phi_f = 0.63$) compared to that of **3** ($\Phi_f = 0.03$), suggesting the cycloaddition of **3** leads an increase in the electron-donating ability in emission of coumarin. When 1 equiv of Cu^{2+} was added to **COT1** in aqueous solution, a dramatic fluorescence quenching was observed (23.6-fold). This could be attributed to the photoinduced electron transfer (PET)[15] from the coumarin fluorophore to the chelated Cu^{2+}. The association constant of **COT1** with Cu^{2+} was determined to be 7.9×10^5 M^{-1} on the basis of the fluorescence titration experiments (Figure S4; see the Supporting Information). The fluorescence intensity increased

(8) (a) Lim, M. H.; Lippard, S. J. *Acc. Chem. Res.* **2007**, *40*, 41–51. (b) Hilderbrand, S. A.; Lim, M. H.; Lippard, S. J. *J. Am. Chem. Soc.* **2004**, *126*, 4972–4978. (c) Tonzetich, Z. J.; McQuade, L. E.; Lippard, S. J. *Inorg. Chem.* **2010**, *49*, 6338–6348. (d) Marti, M. A.; Bari, S. E.; Estrin, D. A.; Doctorovich, F. *J. Am. Chem. Soc.* **2005**, *127*, 4680–4684. (e) Tennyson, A. G.; Do, L.; Smith, R. C.; Lippard, S. J. *Polyhedron* **2007**, *26*, 4625–4630.

(9) Rosenthal, J.; Lippard, S. J. *J. Am. Chem. Soc.* **2010**, *132*, 5536–5537.

(10) (a) Smith, R. C.; Tennyson, A. G.; Lim, M. H.; Lippard, S. J. *Org. Lett.* **2005**, *7*, 3573–3575. (b) Do, L.; Smith, R. C.; Tennyson, A. G.; Lippard, S. J. *Inorg. Chem.* **2006**, *45*, 8998–9005.

(11) McQuadea, L. E.; Ma, J.; Lowe, G.; Ghatpande, A.; Gelperin, A.; Lippard, S. J. *Proc. Natl. Acad. Sci. U.S.A.* **2010**, *107*, 8525–8530.

(12) (a) Lim, M. H.; Xu, D.; Lippard, S. J. *Nat. Chem. Biol.* **2006**, *2*, 375–380. (b) Lim, M. H.; Wong, B. A.; Pitcock, W. H., Jr.; Mokshagundam, D.; Baik, M. H.; Lippard, S. J. *J. Am. Chem. Soc.* **2006**, *128*, 14364–14373. (c) Pluth, M. D.; McQuade, L. E.; Lippard, S. J. *Org. Lett.* **2010**, *12*, 2318–2321.

(13) (a) Trenor, S. R.; Shultz, A. R.; Love, B. J.; Long, T. E. *Chem. Rev.* **2004**, *104*, 3059–3077. (b) Lim, N. C.; Schuster, J. V.; Porto, M. C.; Tanudra, M. A.; Yao, L.; Freake, H. C.; Bruckner, C. *Inorg. Chem.* **2005**, *44*, 2018–2030. (c) Ray, D.; Bharadwaj, P. K. *Inorg. Chem.* **2008**, *47*, 2252–2254. (d) Maity, D.; Govindaraju, T. *Inorg. Chem.* **2010**, *49*, 7229–7231. (e) Yuan, L.; Lin, W.; Song, J. *Chem. Commun.* **2010**, *46*, 7930–7932.

(14) (a) Boren, B. C.; Narayan, S.; Rasmussen, L. K.; Zhang, L.; Zhao, H.; Lin, Z.; Jia, G.; Fokin, V. V. *J. Am. Chem. Soc.* **2008**, *130*, 8923–8930. (b) Sivakumar, K.; Xie, F.; Cash, B. M.; Long, S.; Barnhill, H. N.; Wang, Q. *Org. Lett.* **2004**, *6*, 4603–4306.

(15) (a) Chen, X.; Nam, S. W.; Kim, G. H.; Song, N.; Jeong, Y.; Shin, I.; Kim, S. K.; Kim, J.; Park, S.; Yoon, J. *Chem. Commun.* **2010**, *46*, 8953–8955. (b) Royzen, M.; Dai, Z.; Canary, J. W. *J. Am. Chem. Soc.* **2005**, *127*, 1612–1613.

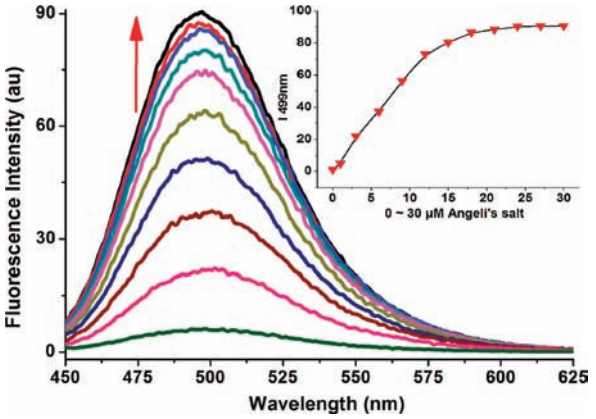

Figure 1. Fluorescence titration of Cu(II)-**COT1** (1 μM) in HEPES buffer (50 mM, 0.1 M KNO_3, pH 7.4) in the presence of different amounts of Angeli's salt. The fluorescence intensity was measured 20 min after the addition of $Na_2N_2O_3$ with excitation at 415 nm. Inset: fluorescence intensity at 499 nm as a function of $Na_2N_2O_3$ concentration.

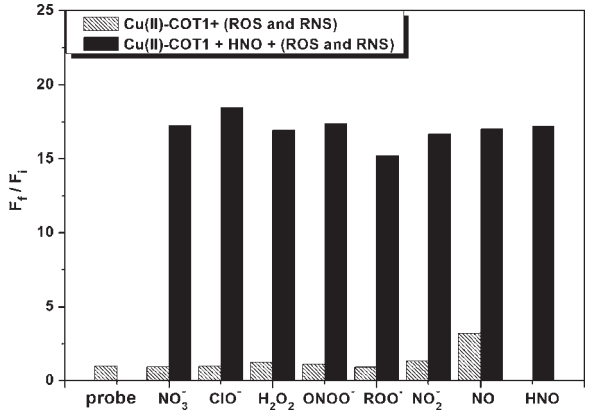

Figure 2. Fluorescence responses of Cu(II)-**COT1** (1 μM) to various 10 μM ROS and RNS species (2 mM for saturated NO aqueous solution). Bars represent the final (F_f) over the initial (F_i) integrated emission at 499 nm. Spectra were acquired in HEPES buffer (50 mM, 0.1 M KNO_3, pH 7.4) solutions. The gray bars represent the addition of the competing ROS or RNS to a 1 μM solution of Cu(II)-**COT1**. The black bars represent the change of the emission that occurred upon the subsequent addition of 20 μM $Na_2N_2O_3$ to the above solutions.

steadily with increasing $Na_2N_2O_3$ concentration (Figure 1) until it reached a plateau at 20 μM $Na_2N_2O_3$, which corresponded to a 17.2-fold increase in fluoresence instensity compared to the blank [HNO]. This indicates that complete reduction of Cu(II)-**COT1** occurred with 20 μM $Na_2N_2O_3$. The HNO induced a dramatic change at 499 nm in the fluorescence intensity, which was much higher than the result obtained with the early reported BODIPY-based sensor.[9] The fluorescence signal was gradually enhanced until the equilibration showed a steady peak at 499 nm (~8 min; see Figure S5 in the Supporting Information), compared to its analogues (which needed 20 min equilibrium time).[7c]

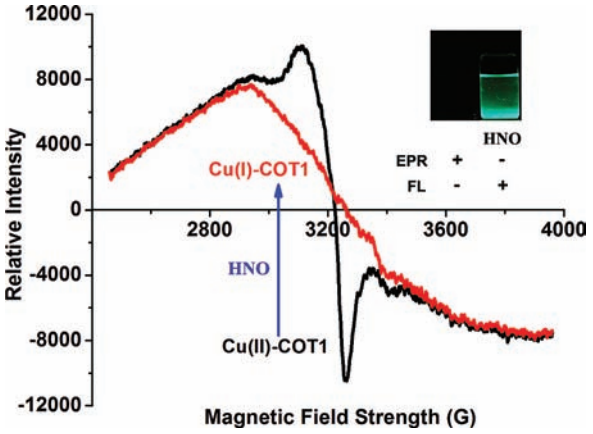

Figure 3. EPR spectra recorded at 298 K for 50 μM Cu(II)-**COT1** in aqueous ethanol (50 mM, pH 7.0, v/v, 50/50) (black line) and with excess $Na_2N_2O_3$ (red line).

Aryl−dipicolylamino (DPA) motifs have been used as components of Zn^{2+} sensors because of their high affinity for Zn^{2+}.[16] Therefore, it was necessary to investigate the effect of Zn^{2+} on the detection of HNO. The addition of $Na_2N_2O_3$ to a Cu(II)-**COT1** solution with excess Zn^{2+} (50 μM) could induce minimal fluorescence intensity changes in comparison with that obtained with HNO alone (Figure S6, see the Supporting Information).

While Cu(II)-**COT1** was highly sensitive to HNO, it was important to investigate its selectivity with various ROS and RNS species (Figure 2). The probe exhibited a 17.2-fold increase with the ratio responses at 499 nm upon interaction with HNO. However, a much weaker response was observed with other biologically relevant ROS and RNS species, including NO_3^-, ClO^-, H_2O_2, $ONOO^-$, $ROO^{\bullet}$, and NO_2^-. With NO, a 3.2-fold increase in fluorescence intensity was observed, and this relative lack of induced fluorescence response could be used to discriminate between NO and HNO. Competitive experiments were conducted with 20 μM $Na_2N_2O_3$ and various ROS and RNS. The fluorescence intensity did not vary much in comparison with that produced by HNO + Cu(II)-**COT1**. Furthermore, the response of the probe to HNO could be detected simply by visual inspection (Figure 3). These results indicate that Cu(II)-**COT1** displays high selectivity toward HNO over other ROS and RNS species.

The EPR spectra of Cu(II)-**COT1** in aqueous solution showed typical paramagnetism[17] with a symmetric line with $g = 2.10$ (Figure 3). The introduction of excess $Na_2N_2O_3$ to the Cu(II)-**COT1** aqueous solution resulted in a rapid decrease in the EPR signal because of the diamagnetism of the reduced Cu(I)-**COT1**. The reduction of Cu^{2+} was corroborated by the ESI-MS spectra of the probe and

(16) (a) Qian, F.; Zhang, C.; Zhang, Y.; He, W.; Gao, X.; Hu, P.; Guo, Z. *J. Am. Chem. Soc.* **2009**, *131*, 1460–1468. (b) Hanaoka, K.; Kikuchi, K.; Kojima, H.; Urano, Y.; Nagano, T. *J. Am. Chem. Soc.* **2004**, *126*, 12470–12476.

(17) Neuman, N. I.; Perec, M.; Gonzalez, P. J.; Passeggi, M. C. G.; Rizzi, A. C.; Brondino, C. D. *J. Phys. Chem. A* **2010**, *114*, 13069–13075.

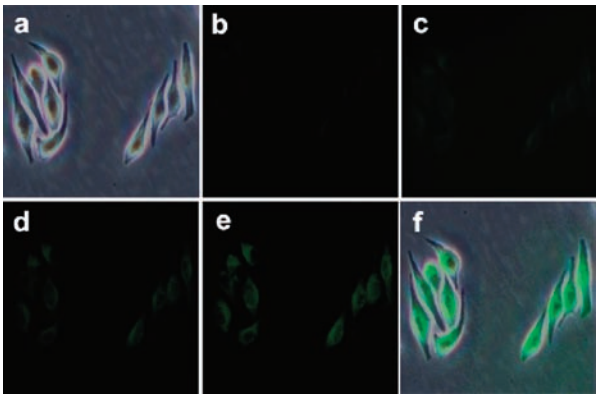

Figure 4. Fluorescence images of A375 cells: (a) bright-field image of cells shown in panel; (b) cells incubated with 5 μM Cu(II)-**COT1** in PBS buffer (50 mM, pH 7.2) for 30 min; (c−e) the cells in (b) incubated with $Na_2N_2O_3$ (50 μM) for 1, 6, and 15, respectively; (f) overlay image of (a) and (e).

Cu(I)-**COT1**. Two major peaks at m/z 558.2 and 616.3 (calcd 558.2 and 616.1) corresponding to [**COT1** + Cu(I)]$^+$ and [**COT1** + Cu(I) + Na + Cl]$^+$ were observed when 5 μM $Na_2N_2O_3$ was added. By comparison, the probe without HNO only exhibited a peak at m/z 593.2 (calcd 593.1), which corresponded to [**COT1** + Cu(II) + Cl]$^+$. In addition, submillimolar cysteine[18] and sodium ascorbate[19] could also be used to restore the typical coumarin green fluorescence (see Figure S7 in the Supporting Information) because of the reduction of chelated Cu(II)-coumarin. A peak for this reduction product was observed in the ESI-MS spectra at m/z 558.2 (calcd 558.2), which corresponded to the cationic [**COT1** + Cu(I)]$^+$ complex.

The probe was then applied to fluorescence imaging of HNO in living cells. Human malignant melanoma A375 cells were first incubated with 5 μM Cu(II)-**COT1** in phosphate-buffered saline for 30 min at 37 °C, which produced very faint intracellular fluorescence (Figure 4b). Then, the treated cells were incubated with 50 μM $Na_2N_2O_3$ and the fluorescence signal was monitored at regular intervals. The signal produced by these cells increased over time (Figure 4c−e). The major fluorescence intensity in the cells was localized in the perinuclear space, which suggests that the NO species did not reach the nucleolus. The overlay of fluorescence and bright-field images indicated that Cu(II)-**COT1** had a good cell membrane permeability. Furthermore, we employed the MTT assay to investigate the cytotoxicity of 5 μM Cu(II)-**COT1** after 12 h of incubation with A375 cells (see theSupporting Information). The Cu(II)-**COT1** probe had low toxicity with the A375 cells, and the tests showed 82.1% cell viability. This low toxicity is important for HNO biological imaging studies.

In summary, a Cu(II) coumarin conjugate probe was developed that acted as a dual-response probe to HNO for both fluorescence and EPR detection. The probe was HNO specific and provided high selectivity over other ROS and RNS species. Great changes in the fluorescence color could be distinguished by the naked eye. Fluorescence imaging shows that Cu(II)-**COT1** could be used for detection of changes in HNO levels in living cells with low cytotoxicity. The design strategy and remarkable photophysical properties of the coumarin green fluorescent moieties will be useful for the development of fluorescent probes for ROS and RNS.

Acknowledgment. This work was supported by the Open Fund of the State Key Laboratory of Materials-Oriented Chemical Engineering (No. KL09-9), the postgraduate practice innovation fund of Jiangsu province, and the doctoral thesis innovation fund of the Nanjing University of Technology.

Supporting Information Available. Text, figures, and a table giving synthesis and experimental details and additional spectroscopic data. This material is available free of charge via the Internet at http://pubs.acs.org.

(18) A reviewer suggested that we investigate the fluorescence intensity change of Cu(II)-**COT1** in the presence of other thiol-containing amino acids; however, we considered that other thiol-containing amino acids have no reduction properties and this work deals with a probe for HNO. Therefore, there is no need to investigate other thiol-containing amino acids.

(19) Taki, M.; Iyoshi, S.; Ojida, A.; Hamachi, I.; Yamamoto., Y. *J. Am. Chem. Soc.* **2010**, *132*, 5938–5939.